

# Lunar Silicon Cavity

Jun Ye,\* Zoey Z. Hu, and Ben Lewis

*JILA, National Institute of Standards and Technology and University of Colorado, Boulder, Colorado 80309-0440, USA*

Wei Zhang

*Jet Propulsion Laboratory, NASA and Caltech, USA*

Fritz Riehle, Uwe Sterr

*Physikalisch-Technische Bundesanstalt, Bundesallee 100, 38116 Braunschweig, Germany*

Yiqi Ni<sup>†</sup> and Julian Struck

*Lunetronic Inc. San Francisco, California 94109, USA*

(Dated: February 9, 2026)

The Moon’s permanently shadowed regions (PSRs) are among the coldest places in the Solar System and are expected to become key landing sites for upcoming international space agency missions. Besides PSRs’ potential rich resources and proximity to perpetual solar power for other scientific and strategic interests, here we present a conceptual development for establishing an unprecedentedly phase-coherent laser. The unique physical environment of lunar PSRs greatly benefits the construction of a cryogenic monolithic silicon cavity that exhibits low  $10^{-18}$  thermal noise-limited stability and coherence time exceeding 1 minute, more than a decade better than the current best terrestrial system. Such a stable laser will serve many applications, including establishing a lunar time standard, building long-baseline optical interferometry, distribution of stable optical signals across a large network of satellites, and forming the backbone for space-based quantum networks.

Aspirations for developing and deploying space-borne quantum technologies can in large part be facilitated by having access to ultrastable lasers that are key to driving and interconnecting optically active quantum systems. On the ground, stable optical local oscillators play many versatile roles in, for example, state-of-the-art optical atomic clocks [1–7], precision test of fundamental physics [8–10], long-baseline optical interferometry including gravitational wave detection [11–13], and optical networks for both classical and quantum information [14, 15]. Cryogenic silicon cavities enable the best performing frequency-stable lasers, with fractional frequency stability of low  $10^{-17}$  and an ultralow linear drift rate of mid  $10^{-20}/\text{s}$  [16, 17]. Permanently shadowed regions (PSRs) on the Moon offer low-temperature and ultra-high vacuum conditions in combination with exceptionally low vibrational noise. This environment is ideal for supporting an ultrastable optical cavity with performance surpassing the best terrestrial systems. Having access to a master optical oscillator frequency stabilized to the lunar cavity forms the basic infrastructure for a range of space-borne experiments, with a cascade of satellites housing either secondary lasers or atomic quantum systems networked together via phase stable optical links.

Lunar PSRs are the chosen landing sites for the NASA-led Artemis mission and other international missions due to their likely resource richness that includes water ice, carbon dioxide and helium-3 [18], as well as continuous solar power at nearby peaks of eternal light [19–21]. However, landing and navigating near PSRs face significant technical challenges. The low Sun elevation angles and

extended shadows limit optical and terrain-relative navigation capability, making precision positioning, navigation, and timing (PNT) essential for safely landing payloads and crewed missions.

We propose to construct a cryogenic silicon cavity located in a PSR to take advantage of the uniquely beneficial physical conditions for such an optical reference cavity. PSRs’ ambient cryogenic temperature and easy access to radiative cooling from deep space permit a simple and passive cooling strategy to reach a zero of the silicon cavity’s thermal expansion coefficient at 17 K. The extreme thermal stability from isolation of solar radiation will enable exceptional long term frequency stability of the optical oscillator. The lunar seismic noise is orders of magnitude lower than in a terrestrial laboratory environment, facilitating robust performance for an extended cavity length to scale down the fundamental Brownian thermal noise contribution. The high vacuum environment of PSRs also eases the construction requirement for a cavity chamber. Overall, once the silicon cavity material is transported to the Moon, the final system engineering will be straightforward to implement and yet with far greater performance prospects.

A highly phase-coherent lunar master laser can serve many important tasks for emerging scientific and technological explorations via space-borne experiments [22–26]. In the absence of atmospheric perturbation, it will be much easier to establish a lunar-space optical link than starting with a stable oscillator on Earth. The lunar laser’s phase stability can thus be transferred with high fidelity to secondary systems on board of various satellite

clusters/constellations, enabling the construction of long baseline space-borne optical interferometers. Each satellite with a laser onboard can have its optical field phase locked to the lunar master laser, greatly simplifying onboard frequency control systems for networks of satellites used for classical or quantum communications, as well as for navigation and flight formation needs. State-of-the-art atomic clocks rely on high-performance and robust local oscillators. The stability of the clock is often determined by the phase coherence of the driving laser. Housing a stable optical reference cavity onboard a satellite to accompany its atomic payload remains a technically sophisticated task. With phase-stable optical links established between satellites and the lunar laser base, any onboard atomic systems can be quickly turned into optical atomic clocks, and benefit from the unmatched phase coherence of the lunar laser.

Another natural outcome following the lunar stable laser is the foundation for an optical atomic clock for lunar time standard [27–29]. The lunar silicon cavity's exceptional long-term frequency stability is, by itself, sufficient for a wide range of applications. With performance below  $10^{-15}$  at a 1 day timescale, the silicon cavity can easily provide a reference for any PNT requirements, and form the backbone of Lunar Coordinated Time (LTC) [29–31]. However, to gain even greater long-term stability, an atomic standard could be added. Only very low-frequency steering would be required, allowing the atomic standard to be located anywhere within the network connected to the cavity.

This proposal thus addresses a critical need for establishing a standalone LTC serving as the cornerstone of the future PNT infrastructure of the Moon. The success of this mission will mark a historic milestone, demonstrating humanity's capability to build fundamental quantum infrastructure on another celestial body, alongside establishing a permanent presence on the Moon. This achievement can have profound implications for future Mars and deep-space missions, where terrestrial timing infrastructure is nearly impossible to access, making the establishment of a standalone local time reference the only viable solution [32].

## PSR ENVIRONMENT CHARACTERISTICS

The Moon's spin axis is nearly perpendicular to its orbital plane around the Sun, causing craters near lunar poles to remain in permanent shadow. These regions, known as PSRs, have eluded sunlight for billions of years. Combined with the lack of internal heating from the Moon's inactive core and low residual heat, PSRs are among the coldest known locations in the entire Solar System. Over time, large amounts of volatile compounds, such as water ice, helium, and carbon dioxide, have been trapped within PSRs. Mining and utilizing

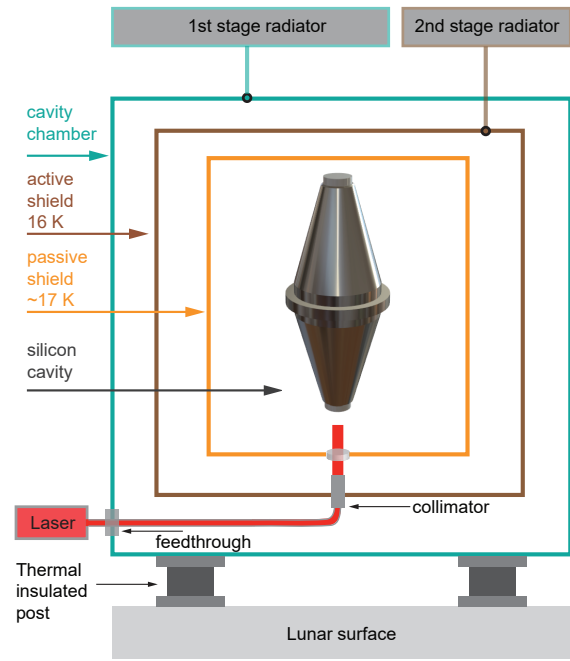


FIG. 1. Conceptual design of a cryogenic silicon cavity based on radiative cooling. The whole system supported by the thermal insulated posts is constructed on the lunar surface. Two radiators, both facing the deep space, provide cooling for an outer radiation shield and an inner actively controlled thermal shield for a 17 K operating temperature where the silicon thermal expansion coefficient is zero. A continuous-wave laser is sent into the cavity chamber via a fiber-optic feedthrough or free-space motorized mirrors and coupled to the silicon cavity with a collimator.

these resources is critical for ongoing deep space exploration, enabling the Moon to serve as a sustainable commercial human base, a refueling outpost, and a testbed for technologies before deploying them to other planets such as Mars.

However, landing payloads near PSRs presents major challenges. In the absence of a terrestrial-like global navigation satellite system, vision-based landing remains one of the few reliable navigation methods. Yet, because the solar incidence angle near PSRs is nearly parallel to the surface, objects cast extremely long shadows, creating significant obstacles for precision lunar landing. A local timescale will solve this problem.

We summarize that the PSRs environment (Table I) is ideal for deploying a cryogenic silicon cavity-based timescale, close to future permanent human bases, utilizing the naturally maintenance-free conditions of PSRs.

## Temperature

The thermal environment of the south polar PSRs has been monitored for over a decade through remote sensing

by NASA’s Lunar Reconnaissance Orbiter, ranging from about 20 K in winter to 60 K in summer [33]. Seasonal variations are primarily driven by the Moon’s 1.5° axial tilt relative to the Earth-Sun orbital plane. Owing to the slow motion of this tilt and the extreme isolation of PSRs, temperature changes are both gradual and highly predictable, approximately 50 mK per day.

### Radiative cooling

For cooling and thermal stabilization of the silicon cavity, we will engineer access to deep space radiative cooling. This passive cooling method is free of vibration and cryogen and has been widely used in space missions, such as James Webb Space Telescope [34, 35] and far-side seismic suite [36]. Figure 1 illustrates the conceptual design of the cavity system on the lunar surface. Similar to systems currently operated in the lab, three layers of thermal shields are provided for the silicon cavity. The cavity chamber connected to the first radiator is cooled down to 30–40 K. The active shield attached to the second radiator is approximately 16 K, controlled by an active temperature servo. To accommodate the PSR’s temperature cycle of 20–60 K from winter to summer, a thermal switch [36] will be used to adjust the first radiator’s cooling power, to keep the heating power needed for the active shield below 0.25 W. The passive shield provides a long time constant for thermal equilibrium of the silicon cavity, which is stabilized at the zero-crossing of the coefficient of thermal expansion at approximately 17 K. This fully passive cooling strategy relies on the natural cryogenic environment of the Moon and deep space (2.7 K).

### Vacuum

The Moon’s weak gravity prevents it from retaining a substantial atmosphere, resulting in a naturally maintained ultra-high vacuum environment. Direct measurements from the Apollo missions recorded surface neutral particle pressure of about  $10^{-6}$  Pa during the lunar day and  $10^{-10}$  Pa at night [37]. Since the primary source of residual gas on the Moon is solar wind interaction, the vacuum within PSRs is expected to be even lower. This inference is supported by the persistence of volatile compounds, such as water ice, that have remained stable in PSRs cold traps for billions of years.

### Ground Vibration

The absence of a lunar atmosphere eliminates above-ground acoustic noise, and the Moon exhibits an exceptionally low seismic background compared to Earth due

to its minimal tectonic activity. Multiple Apollo missions directly measured the lunar seismic background [38–43]. In the absence of moonquakes, the ambient ground vibration was found to be below the seismometer noise floor, approximately 0.3 nm at 1 Hz, significantly quieter than any known site on Earth [39]. Moon ground vibration can be caused by four major events, deep moonquake, shallow moonquake, thermal moonquake, and meteor impacts [44, 45]. Thermal moonquakes are the most common, caused by thermal expansion and contraction between lunar day and night, where surface temperatures can fluctuate by up to 300 K. The average amplitude of thermal moonquakes is about 0.6 nm, with peak values around 6 nm, substantially quieter than a typical Earth-based scientific laboratory [46]. Because the thermal environment within PSRs is far more stable than at the Apollo landing sites, significantly fewer thermal moonquakes are expected inside PSRs. Deep and shallow moonquakes may be induced by tidal stresses from Earth, while meteoroid impacts can occasionally generate localized seismic disturbances [47, 48]. In general, the Moon’s seismic noise background is about four orders of magnitude lower than even the quietest continental sites on Earth [49], making it an ideal environment for silicon-cavity-based optical clocks.

The combined conditions of the stable cryogenic thermal environment of the PSR, ultra-high vacuum, and intrinsically low ground vibration create an ideal natural infrastructure to deploy silicon-cavity-based optical clocks as an independent reference for lunar time, as well as other quantum instruments in the future. We propose a low-size, weight, and power (SWaP) architecture that requires minimal to zero active thermal management to realize an ultra-stable timing node for synchronizing lunar assets.

TABLE I. PSR Environment. The temperature range corresponds to remote measurements of a Haworth Crater site. The vacuum pressure is projected based on the Apollo mission data taken in lunar equatorial regions [37]. The vacuum pressure is expected to be significantly lower in PSRs. The PSR ground vibration is evaluated at Fourier frequency of 1 Hz, with the maximum vibration level associated with artificial impacts of Saturn IVB rocket stages during Apollo [49].

Property	Average	Min	Max
Temperature (K)	< 0.05/day drift	< 20	60
Vacuum (Pa)	$< 10^{-10}$		
Vibration (m/s <sup>2</sup> )	$< 1.2 \times 10^{-8}$	$< 1.2 \times 10^{-8}$	$3 \times 10^{-6}$

## SILICON CAVITY PROPERTIES

We now connect the favorable environmental conditions of PSRs to the physical properties of silicon cavities to highlight the potential for improving their frequency stability beyond what is available in the ground laboratory today. The low vibration background will reduce high frequency noise associated with the optical cavity. Thermal stability and abundance of the cooling power provide long term stability at zero crossing of the silicon crystal's thermal expansion coefficient. Considering the high vacuum surroundings at PSRs, only a modest shielding chamber is needed to protect the silicon cavity and ensure that the background pressure fluctuation within the optical cavity is below  $10^{-10}$  Pa.

We illustrate the tradeoff between performance and system size by comparing two designs. A 21 cm cavity follows the current design of silicon cavities in the lab. A longer cavity of 50 cm length will be more sensitive to the vibration noise, but the PSR's low vibration environment significantly reduces this concern. The longer 50 cm cavity reduces the fundamental Brownian thermal noise of the mirror coatings and enlarges the optical mode area. For ultimate performance, we can also use mirror coatings based on stacks of crystalline GaAs/AlGaAs for lower thermal noise than conventional dielectric mirrors.

Table II shows the thermal noise floor of these cavity designs, which are all below  $10^{-17}$ , a significant improvement over the state-of-the-art performance of  $\sim 3 \times 10^{-17}$  for terrestrial-based cryogenic silicon cavities. We assume the use of one plano mirror and one with a 10 m radius of curvature. Of course, the overall performance of the lunar cavity will also include contributions from other noise sources, including optical beam propagation stability, intracavity gas/vacuum noise, residual amplitude noise in frequency modulation, and so on. However, a stable environment offered by PSRs will correspondingly reduce the magnitude of all these noise contributions.

TABLE II. Thermal noise levels for different cavity designs. Longer cavities and crystalline coatings reduce the noise level.

Cavity Design		
Length	Coating	Thermal noise
21 cm	Conventional	$9 \times 10^{-18}$
21 cm	Crystalline	$2 \times 10^{-18}$
50 cm	Conventional	$3 \times 10^{-18}$
50 cm	Crystalline	$8 \times 10^{-19}$

## Thermal Management

To maintain the silicon cavity at a 17 K operating temperature, we estimate the thermal load based on the following conditions. The surface of the cavity chamber, active shield, and passive shield are gold-coated to ensure low emissivity (5%) between different layers. Each layer may be mounted using high strength and low thermal conductivity cables, e.g. Kevlar fiber [50]. The whole system is supported by thermally insulated posts. The coupling to external blackbody radiation is minimized by using a fiber-optic feedthrough. The use of the two separate radiators, as outlined in Fig. 1, makes it practical to support a silicon cavity with relatively long length (50 cm and biconical as shown in Fig. 1). The size of the first radiator is  $10\text{--}20 \text{ m}^2$ , and the second radiator is  $1\text{--}10 \text{ m}^2$ . Note that this radiator design includes a conservative margin of 50% higher heating load than a realistic estimate.

## Seismic Noise

The most recent 21 cm silicon cavity has measured acceleration sensitivities of  $1 \times 10^{-10}/g$  and  $3 \times 10^{-11}/g$  for two orthogonal horizontal directions, and  $1.5 \times 10^{-11}/g$  for the vertical direction [51]. Here,  $g = 9.8 \text{ m/s}^2$  is the gravitational acceleration on the surface of the Earth. We only have data for the Moon's vibrational noise in the vertical direction, and we expect the horizontal vibrational noise to be much lower than the vertical noise. We can compare the expected vibration-induced noise for a lunar cavity and a terrestrial cavity that are mounted on an actively vibration-isolated table, see Fig. 2. The Moon's passive noise, with no isolation, is less than that of an active isolation system on Earth. If horizontal noise is comparable to vertical noise, its effect would be larger due to the higher horizontal sensitivity; nevertheless, it would still be below the  $1 \times 10^{-18}$  level for frequencies below 1 Hz. The 50 cm cavity would have a higher vibration sensitivity, potentially by a factor of 5, placing the vibration noise-induced fractional frequency fluctuation around  $1 \times 10^{-18}$ . Because the cavity is passively cooled, the cooling system does not induce vibrations, as would happen on Earth. Overall, we expect the vibration-induced noise to be below the fundamental thermal noise of the cavity.

## Vacuum Pressure

Residual gas within the spacer hole modifies the effective optical path length through pressure- and temperature-dependent refractive index variations. In the terrestrial lab, refractive index fluctuations in air

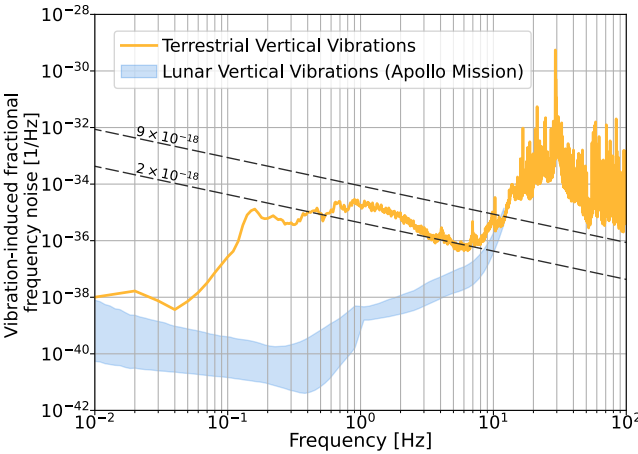


FIG. 2. Comparison of terrestrial and lunar vibration-induced fractional frequency noise. The blue shaded region denotes lunar seismic vibration noise in the vertical direction) from the Apollo missions, scaled by the measured vertical acceleration sensitivity of the 21 cm cavity ( $1.5 \times 10^{-11}/g$ ), and spanning the 10th to 90th percentile range. These data were constructed and analyzed by [41] from multiple Apollo stations operated in both flat-response and peak-mode seismometer configurations. The orange trace shows an example of typical terrestrial laboratory vibration conditions with considerable vibration control effort. The dashed lines indicate the thermal noise levels for the 21 cm cavity with conventional and crystalline coatings respectively.

have been well characterized with the Edlén equation [52], which allows the estimation of the vacuum stability required to reach the expected thermal noise limited performance. At 17 K, the fractional frequency varies with pressure  $\sim 4 \times 10^{-8}/\text{Pa}$ , assuming that the refractivity per unit density of the residual gas is similar to that of air. For the recent 21 cm terrestrial cavity operated at 17 K, a steady-state pressure of  $10^{-7} \text{ Pa}$  is reached with active pumping, and its fluctuation is estimated to be  $\leq 1 \times 10^{-10} \text{ Pa}$  for a stability limit of  $5 \times 10^{-18}$ .

In contrast, lunar PSRs have naturally extensive cold surfaces that passively suppress the overall vacuum levels and minimal diurnal variation [54–56]. As mentioned previously, direct measurements from the Apollo missions reported a surface neutral particle pressure of  $1 \times 10^{-10} \text{ Pa}$  level at night [37]. These data, not collected within PSR regions, provide a conservative upper bound for expected local pressure level and temporal pressure activities: some of the gases probably condense/adhere to the significantly colder surfaces in the PSRs and their thermal stability guarantees pressure stability since there is no gas desorption cycle related to illumination. Therefore, the local pressure and temporal fluctuations in the PSRs are expected to remain well below the level required thermal noise limited stability performance without the need for an active pump. There are obvious risk fac-

tors that need to be mitigated, including the shielding of lunar dust, ionizing radiation, and micrometeorites.

## APPLICATIONS OF THE LUNAR SILICON CAVITY/OUTLOOK

A wide range of applications, from fundamental physics to practical communication and navigation needs, will be enabled by a lunar silicon-cavity-based laser system. As shown in Fig. 3, with a simple heterodyne beat and optical phase locking setup, the silicon cavity’s optical stability can be transferred to a high power laser located on the ridge of PSRs with permanent solar energy, and subsequently connected to an array of satellites that house atomic standards, optical interconnects, interferometric components, and long-baseline capabilities to reach back to Earth.

This stable laser will allow for establishment of a lunar optical atomic clock. The ultrastable silicon cavity already provides sufficiently high stability, with performance that could surpass maser [57]. The free-running cavity frequency can provide a stand-alone frequency/phase reference to many demanding applications. If steered by an atomic standard on a regular basis with relatively low duty cycles, the system will provide an optical time scale [57–61]. The atomic standard can be located on the Moon, or on a satellite, with an optical link between the Moon and the satellite, to provide maximum flexibility. Together with the optical frequency comb technology, multiple atomic standards may take advantage of this lunar infrastructure. Such a network of frequency steered and interconnected satellites will greatly aid communication and navigation needs between Earth and the Moon [27, 62]. Since a precise time reference underpins the PNT, this network will strengthen the resilience of the lunar mission by enabling networked communications, the collection of correlated scientific data and safe landing, even during long holdover periods without terrestrial signals [63].

Ultrastable space-based optical oscillators will also become widely available. Each satellite no longer needs to be equipped with its own cavity-based frequency stabilization device. The lunar silicon cavity can serve as the common reference for connecting satellites, each housing a receiver and potentially a phase locked loop to track the incoming optical phase. A two-way optical frequency/phase transfer can be established between pairs of satellites, as well as between the Moon and satellites. This infrastructure will thus play a valuable role in establishing a space-based long baseline optical interferometer for deep space imaging, astronomical observation, and gravitational wave detection. With the Moon’s orbit determined at the few-millimeter level [64], this stable gravitational system also enables unique tests of general relativity. The exquisite silicon cavity at this unique lo-

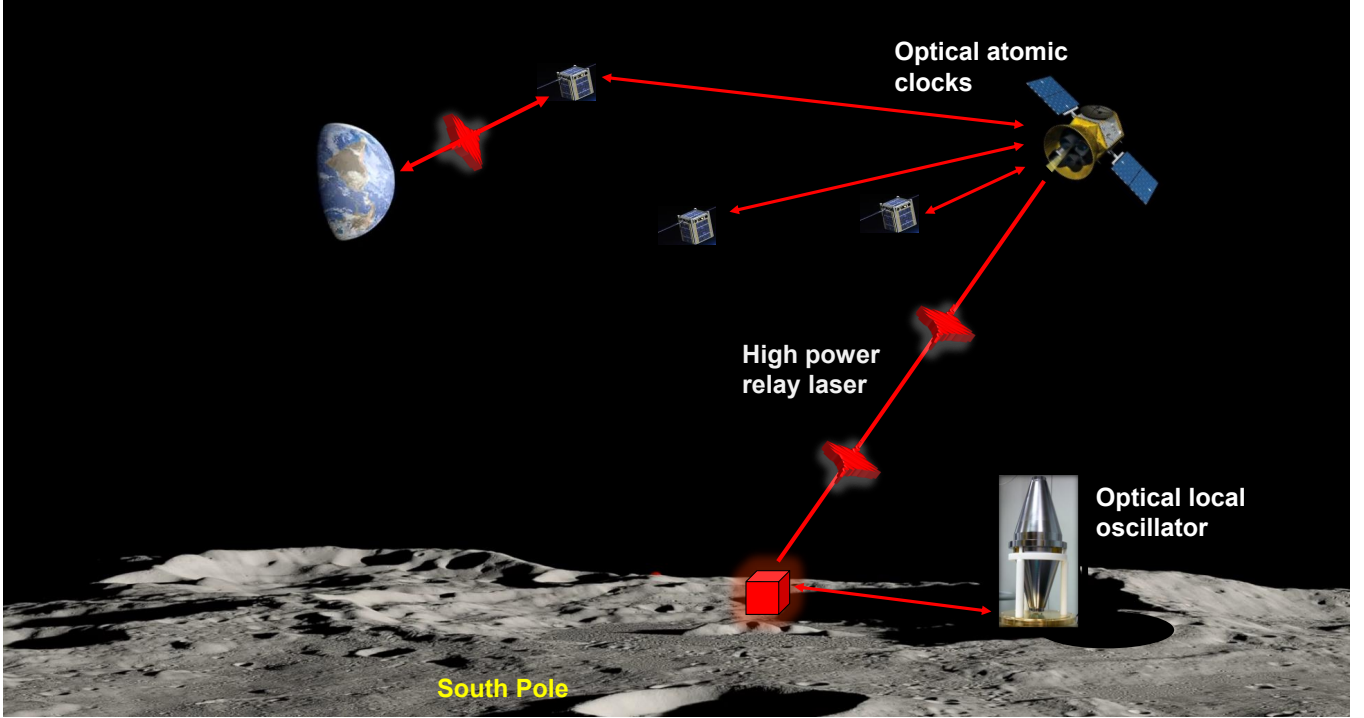


FIG. 3. Application of a lunar PSR silicon cavity as the basic infrastructure for lunar time scale, Earth-Moon optical communication, satellite-based space interferometry and imaging, and networking to Earth-bound time scale. Lunar PSR background image produced by NASA's visualization studio [53].

cation can enable investigations of fundamental interaction of the cavity itself, such as for mHz gravitational wave detection [65] or observation of the effects of dark matter on solids [66]. The distance between Earth and the Moon is only one light-second. The silicon cavity's optical coherence time far exceeds this time scale, and ultimately the ultrastable optical frequency reference, as well as the atomic standard-steered lunar optical time scale, can reach terrestrial labs on Earth through free-space optical links, which can provide a global network for clock synchronization among national metrology labs across continents.

We thank J. L. Hall, D. Lee, I. Mckinley, and J. K. Thompson for technical discussions and useful feedback on the manuscript. The work is supported by NIST, NSF, VBFF, the Moore/Simons Foundation, and NASA/JPL's Strategic University Research Partnerships (SURP) program. F.R. and U.S. acknowledge support from Germany's Excellence Strategy EXC-2123 QuantumFrontiers (Project No. 390837967).

Y. Ni and J. Struck are with Lunetronic, which is designing future quantum infrastructure inside lunar permanently shadowed regions (PSRs). The other authors declare no competing interests.

\* ye@jila.colorado.edu

† yiqi@lunetronic.com

- [1] D. G. Matei, T. Legero, S. Häfner, C. Grebing, R. Weyrich, W. Zhang, L. Sonderhouse, J. M. Robinson, J. Ye, F. Riehle, and U. Sterr, *Phys. Rev. Lett.* **118**, 263202 (2017).
- [2] E. Oelker, R. B. Hutson, C. J. Kennedy, L. Sonderhouse, T. Bothwell, A. Goban, D. Kedar, C. Sanner, J. M. Robinson, G. E. Marti, D. G. Matei, T. Legero, M. Giunta, R. Holzwarth, F. Riehle, U. Sterr, and J. Ye, *Nat. Photonics* **13**, 714 (2019).
- [3] T. Bothwell, W. Brand, R. Fasano, T. Akin, J. Whalen, T. Grogan, Y.-J. Chen, M. Pomponio, T. Nakamura, B. Rauf, I. Baldoni, M. Giunta, R. Holzwarth, C. Nelson, A. Hati, F. Quinlan, R. Fox, S. Peil, and A. D. Ludlow, *Opt. Lett.* **50**, 646 (2025).
- [4] M. C. Marshall, D. A. Rodriguez Castillo, W. J. Arthur-Dworschack, A. Aepli, K. Kim, D. Lee, W. Warfield, J. Hinrichs, N. V. Nardelli, T. M. Fortier, J. Ye, D. R. Leibrandt, and D. B. Hume, *Phys. Rev. Lett.* **135**, 033201 (2025).
- [5] R. Hobson, W. Bowden, A. Vianello, A. Silva, C. F. A. Baynham, H. S. Margolis, P. E. G. Baird, P. Gill, and I. R. Hill, *Metrologia* **57**, 065026 (2020).
- [6] A. Tofful, C. F. A. Baynham, E. A. Curtis, A. O. Parsons, B. I. Robertson, M. Schioppo, J. Tunisi, H. S. Margolis, R. J. Hendricks, J. Whale, R. C. Thompson, and R. M.

Godun, *Metrologia* **61**, 045001 (2024).

[7] S. B. Koller, J. Grotti, S. Vogt, A. Al-Masoudi, S. Dörscher, S. Häfner, U. Sterr, and C. Lisdat, *Phys. Rev. Lett.* **118**, 073601 (2017).

[8] C. Braxmaier, H. Müller, O. Pradl, J. Mlynek, A. Peters, and S. Schiller, *Phys. Rev. Lett.* **88**, 010401 (2002).

[9] J. Sanjuan, K. Abich, M. Gohlke, A. Resch, T. Schultdt, T. Wegehaupt, G. P. Barwood, P. Gill, and C. Braxmaier, *Opt. Express* **27**, 36206 (2019).

[10] T. Bothwell, C. J. Kennedy, S. Yu, D. Kedar, J. M. Robinson, E. Oelker, E. Staron, and J. Ye, *Nature* **602**, 420 (2022).

[11] I. Pikovski, M. R. Vanner, M. Aspelmeyer, M. S. Kim, and Č. Brukner, *Nature Physics* **8**, 393 (2012).

[12] T. E. Mehlstäubler, G. Grosche, C. Lisdat, P. O. Schmidt, and H. Denker, *Rep. Prog. Phys.* **81**, 064401 (2018).

[13] G. Barontini, X. Calmet, V. Guarnera, A. Smith, and A. Vecchio, *Class. Quantum Grav.* **10.1088/1361-6382/ae09ec** (2025).

[14] N. V. Nardelli, D. V. Reddy, M. Grayson, D. Sorensen, M. J. Stevens, M. D. Mazurek, L. K. Shalm, and T. M. Fortier, Phase-stable optical fiber links for quantum network protocols, arXiv:2510.16230 (2025).

[15] F. Riehle, *Nature Photonics* **11**, 25 (2017).

[16] D. Lee, Z. Hu, B. Lewis, A. Aeppli, K. Kim, Z. Yao, T. Legero, D. Nicolodi, F. Riehle, U. Sterr, and J. Ye, *Phys. Rev. Lett.* **136**, 033801 (2026).

[17] T. Kessler, C. Hagemann, C. Grebing, T. Legero, U. Sterr, F. Riehle, M. J. Martin, L. Chen, and J. Ye, *Nature Photonics* **6**, 687 (2012).

[18] D. A. Paige, M. A. Siegler, J. A. Zhang, P. O. Hayne, E. J. Foote, K. A. Bennett, A. R. Vasavada, B. T. Greenhagen, J. T. Schofield, D. J. McCleese, M. C. Foote, E. DeJong, B. G. Bills, W. Hartford, B. C. Murray, C. C. Allen, K. Snook, L. A. Soderblom, S. Calcutt, F. W. Taylor, N. E. Bowles, J. L. Bandfield, R. Elphic, R. Ghent, T. D. Glotch, M. B. Wyatt, and P. G. Lucey, *Science* **330**, 479 (2010).

[19] D. B. J. Bussey, P. D. Spudis, and M. S. Robinson, *Geophys. Res. Lett.* **26**, 1187 (1999).

[20] V. T. Bickel, B. Moseley, I. Lopez-Francos, and M. Shirley, *Nature Commun.* **12**, 5607 (2021).

[21] D. J. Ben Bussey, P. G. Lucey, D. Steutel, M. S. Robinson, P. D. Spudis, K. D. Edwards, P. G. Lucey, D. Steutel, M. S. Robinson, P. D. Spudis, and K. D. Edwards, *Geophys. Res. Lett.* **30**, 1278 (2003).

[22] S. Kolkowitz, I. Pikovski, N. Langellier, M. D. Lukin, R. L. Walsworth, and J. Ye, *Phys. Rev. D* **94**, 124043 (2016).

[23] S. G. Turyshev, *Phys. Rev. Appl.* **23**, 064066 (2025).

[24] X.-Q. Zhu, X.-M. Zhai, Y. Xie, Y. Miao, H.-W. Yu, D.-Q. Kong, W.-L. Song, Y.-W. Zhang, Y. Hu, X.-Y. Cui, X. Jiang, B.-Y. Yang, J.-J. Jia, J. Yin, S.-K. Liao, R. Shu, C.-Z. Peng, P. Xu, H.-N. Dai, Y.-A. Chen, and J.-W. Pan, *Optica* **12**, 1342 (2025).

[25] S. M. Kopeikin and G. H. Kaplan, *Phys. Rev. D* **110**, 084047 (2024).

[26] M. Lezius, T. Wilken, C. Deutsch, M. Giunta, O. Mandel, A. Thaller, V. Schkolnik, M. Schiemangk, A. Dinkelaker, A. Kohfeldt, A. Wicht, M. Krutzik, A. Peters, O. Hellmig, H. Duncker, K. Sengstock, P. Windpassinger, K. Lampmann, T. Hülsing, T. W. Hänsch, and R. Holzwarth, *Optica* **3**, 1381 (2016).

[27] P. Berceau, M. Taylor, J. M. Kahn, and L. Hollberg, *Class. Quantum Grav.* **33**, 135007 (2016).

[28] A. Derevianko, K. Gibble, L. Hollberg, N. R. Newbury, C. Oates, M. S. Safronova, L. C. Sinclair, and N. Yu, *Quantum Sci. Technol.* **7**, 044002 (2022).

[29] A. Bourgoin, P. Defraigne, and F. Meynadier, *Metrologia* **63**, 015003 (2026).

[30] N. Ashby and B. R. Patla, *Astronom. J.* **168**, 112 (2024).

[31] A. Fienga, N. Rambaux, and K. Sośnica, Lunar references systems, frames and time-scales in the context of the ESA programme moonlight (2024), arXiv:2409.10043 [physics.space-ph].

[32] E. A. Burt, J. D. Prestage, R. L. Tjoelker, D. G. Enzer, D. Kuang, D. W. Murphy, D. E. Robison, J. M. Seubert, R. T. Wang, and T. A. Ely, *Nature* **595**, 43 (2021).

[33] J. P. Williams, B. T. Greenhagen, D. A. Paige, N. Schorghofer, E. Sefton-Nash, P. O. Hayne, P. G. Lucey, M. A. Siegler, and K. M. Aye, *J. Geophys. Res.: Planets* **124**, 2505 (2019).

[34] R. G. Ross, *Cryocoolers* **22**, 1 (2022).

[35] M. Menzel, M. Davis, K. Parrish, J. Lawrence, A. Stewart, J. Cooper, S. Irish, G. Mosier, M. Levine, J. Pitman, G. Walsh, P. Maghami, S. Thomson, E. Wooldridge, R. Boucarut, L. Feinberg, G. Turner, P. Kalia, and C. Bowers, *Publ. Astron. Soc. Pac.* **135**, 058002 (2023).

[36] A. Aboobaker, M. Panning, and R. Bugby, in *2024 IEEE Aerospace Conference* (Big Sky, USA, 2024) pp. 1–8.

[37] F. S. Johnson, J. M. Carroll, and D. E. Evans, *J. Vac. Sci. Technol.* **9**, 450 (1972).

[38] NASA, Apollo 11 seismic experiment, <https://science.nasa.gov/resource/apollo-11-seismic-experiment/> (2017).

[39] G. V. Latham, M. Ewing, F. Press, G. Sutton, J. Dorman, Y. Nakamura, N. Toksoz, R. Wiggins, J. Derr, and F. Duennebier, *Science* **167**, 455 (1970).

[40] Y. Nakamura, G. V. Latham, and H. J. Dorman, *J. Geophys. Res.* **87**, A117 (1982).

[41] C. Nunn, W. T. Pike, I. M. Standley, S. B. Calcutt, S. Kedar, and M. P. Panning, *Planet. Sci. J.* **2**, 36 (2021).

[42] C. Nunn, N. A. Teamby, J. Wooley, N. Murdoch, and D. Mimoun, *Space Sci. Rev.* **216**, 89 (2020).

[43] J. S. Watkins and R. L. Kovach, *Science* **175**, 175 (1972).

[44] M. N. Toksöz, A. M. Dainty, S. C. Solomon, and K. R. Anders, *Reviews of Geophysics and Space Physics* **12**, 539 (1974).

[45] C. Nunn, R. F. Garcia, Y. Nakamura, A. G. Marusiak, T. Kawamura, D. Sun, L. Margerin, R. Weber, M. Drilleau, M. A. Wieczorek, A. Khan, A. Rivoldini, P. Lognonné, and P. Zhu, *Space Sci. Rev.* **216**, 89 (2020).

[46] F. Duennebier and G. H. Sutton, *J. Geophys. Res.* **79**, 4351 (1974).

[47] J. Majstorović, L. Vidal, and P. Lognonné, *Phys. Rev. D* **111**, 044061 (2025).

[48] G. V. Latham, M. E. Brown, M. A. Nicolich, J. E. Munson, and W. W. Vaughn, *J. Geophys. Res.* **75**, 2660 (1970).

[49] R. D. Lorenz and M. Panning, *Icarus* **303**, 273 (2018).

[50] D. Bugby, B. Marland, C. Stouffer, and E. Kroliczek, *Cryocoolers* **12**, 693 (2003).

[51] B. Lewis, Z. Hu, D. Lee, J. Ye, T. Legero, D. Nicolodi, F. Riehle, and U. Sterr (2026), proceedings of the International Frequency Control Symposium, submitted.

[52] B. Edlén, *Metrologia* **2**, 71 (1966).

[53] NASA Scientific Visualization Studio, Lunar south pole

illumination with Earth and Sun, <https://svs.gsfc.nasa.gov/5228/> (2024), visualizer: Ernie Wright.

[54] D. A. Paige, M. A. Siegler, J. A. Zhang, P. O. Hayne, E. J. Foote, K. A. Bennett, A. R. Vasavada, B. T. Greenhagen, *et al.*, *Science* **330**, 479 (2010).

[55] M. Siegler, D. Paige, J. P. Williams, and B. Bills, *Icarus* **255**, 78 (2015).

[56] J.-P. Williams, D. A. Paige, B. T. Greenhagen, and M. A. Siegler, *J. Geophys. Res.: Planets* **124**, 2505 (2019).

[57] W. R. Milner, G. E. Marti, J. M. Robinson, J. Ye, A. Derevianko, and J. Ye, *Phys. Rev. Lett.* **123**, 173201 (2019).

[58] J. Yao, Q. Liu, R. Hummels, W. G. Lee, E. A. Donley, T. E. Parker, J. Levine, C. W. Oates, J. A. Sherman, and T. M. Fortier, *Phys. Rev. Appl.* **12**, 044069 (2019).

[59] H. Hachisu, F. Nakagawa, Y. Hanado, and T. Ido, *Sci. Rep.* **8**, 4243 (2018).

[60] V. Formichella, F. Levi, D. Calonico, A. Godone, F. Bertacco, S. Micalizio, G. Costanzo, M. Pizzocaro, P. Barbieri, C. Clivati, F. Cappellaro, M. Belmonte, F. Bregolin, B. Garrido, G. Cappellini, M. Caorsi, and M. Schioppo, *Optica* **11**, 523 (2024).

[61] X. Zhang, F.-F. Chang, Y. Huang, J.-F. Cao, X. Jian, H. Sun, R.-S. Zeng, F. Fang, J. Guo, Z. Guo, Y. Jiang, B. Lü, and Y. Yuan, *AIP Adv.* **13**, 115316 (2023).

[62] T. Ely, E. Burt, K. Cheung, and R. Tjoelker, *Radio Sci.* **60**, e2025RS008244 (2025).

[63] D. J. Israel, K. D. Mauldin, C. J. Roberts, J. W. Mitchell, A. A. Pulkkinen, L. V. D. Cooper, M. A. Johnson, S. D. Christe, and C. J. Gramling, in *2020 IEEE Aerospace Conference* (2020) pp. 1–14.

[64] J. B. R. Battat, T. W. Murphy, E. G. Adelberger, B. Gillespie, C. D. Hoyle, R. J. McMillan, E. L. Michelsen, K. Nordtvedt, A. E. Orin, C. W. Stubbs, and H. E. Swanson, *Publ. Astron. Soc. Pac.* **121**, 29 (2009).

[65] G. Barontini, X. Calmet, V. Guarnera, A. Smith, and A. Vecchio, *Class. Quantum Grav.* **42**, 20LT01 (2025).

[66] P. Wcisło, P. Morzyński, M. Bober, A. Cygan, D. Lisak, R. Ciuryło, and M. Zawada, *Nat. Astron.* **1**, 0009 (2016).